Measurement of the Spin Dependent Structure Function $g_1^p(x, Q^2)$ at HERA

R. Ball[a], A. Deshpande[b], S. Forte[c], V. W. Hughes[b], J. Lichtenstadt[d,e], G. Ridolfi[f]

[a] Department of Physics and Astronomy, Edinburgh EH9 3JZ, Scotland
[b] Department of Physics, Yale University, New Haven, CT 06511, USA [1]
[c] INFN , Sezione di Torino, I-10125 Torino, Italy
[d] CERN, CH-1211 Geneva 23, Switzerland
[e] School of Physics and Astronomy, The Raymond and Beverly Sackler Faculty of Exact Sciences, Tel Aviv University, Tel Aviv 69978, Israel [2]
[f] INFN, Sezione di Genova, I-16146, Genova, Italy

Abstract: We present estimates of possible data on spin-dependent asymmetries in inclusive scattering of high energy polarized electrons by high energy polarized protons at HERA, including statistical errors, and discuss systematic uncertainties. We show that these data would shed light on the small x behaviour of the polarized structure function g_1, and would reduce substantially the uncertainty on the determination of the polarized gluon distribution.

1 Introduction

Nucleon structure, particularly as defined by its structure functions determined from lepton-nucleon inclusive electromagnetic scattering, is of fundamental importance and has provided crucial information for the development of perturbative QCD. The history of such experiments over the past forty years has shown that important new information has been obtained when measurements were extended to new kinematic regions. In the mid-1950's at Stanford, Hofstadter [1] extended measurements of elastic electron-proton scattering to a higher Q^2 range of 1 (GeV/c)^2 and first observed that the proton has a finite size. In the late 1960's at SLAC Friedman, Kendall and Taylor [2] extended measurements of inelastic inclusive electron scattering to the deep inelastic region of $Q^2 > 1$ (GeV/c)^2 and discovered the parton substructure of the proton.

The subfield of polarized lepton-proton scattering was initiated with the Yale-SLAC E80 and E130 experiments [3] which measured the spin-dependent structure function of the proton in the mid-1980's. These experiments were then followed up at CERN by the EM Collaboration

[1] Supported by the Department of Energy.
[2] Supported by the Israel Science Foundation of the Israeli Academy of Sciences.

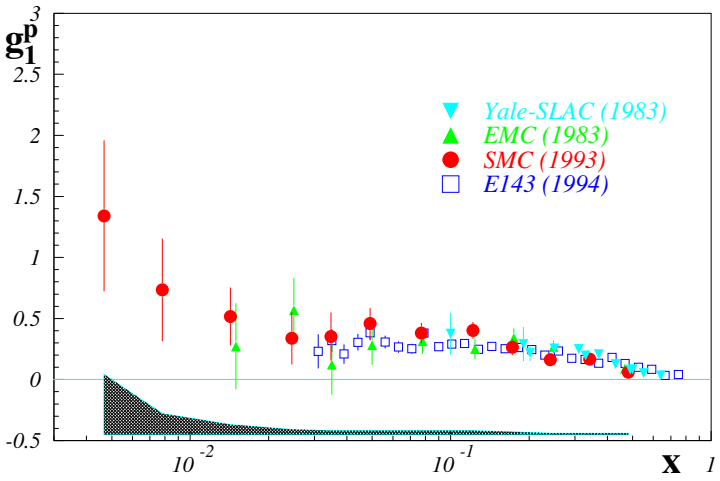

Figure 1: *The current status of the measurement of the spin structure function g_1^p. The statistical errors are shown with the data points, while the size of the systematic errors for SMC measurement is shown by the shaded area.*

which extended the kinematic range of the original measurements at SLAC to lower the x range from $x = 0.1$ to 0.01 [4]. These data allowed a determination of the singlet component of the first moment of g_1, which in the naive parton model is the fraction of the proton spin carried by quarks: this was found to be compatible with zero, thereby violating the parton model Ellis-Jaffe sum rule at the three standard deviation level. This surprising result has stimulated a large amount of experimental and theoretical work on polarized structure functions [5]. New measurements of the spin dependent structure functions of the proton and the deuteron were made by the SM collaboration [6] at CERN and by E143 [7] at SLAC which extended the kinematic range to lower x and also reduced the statistical and systematic uncertainties significantly. Figure 1 shows all published measurements of the structure function g_1^p. These measurements, along with those made for the deuteron, allowed a better determination of the first moment of the spin structure functions and verified the Bjorken sum rule. Furthermore, they made a next-to leading order QCD analysis of the x and Q^2 dependence of g_1 possible, thereby allowing a determination of the first moment of the polarized gluon distribution [8].

In view of this history it is important to consider in detail what measurements and accuracies may be obtained at HERA. The primary goal and motivation for HERA is to extend the kinematic range of electron-proton scattering. Thus far HERA research and its discoveries were the results of the new and vastly extended kinematic range in x and Q^2 , both by a factor of about 100, provided by the collider [9, 10, 11, 12]. At present the 800 GeV proton beam at HERA is unpolarized (although the 25 GeV electron/positron beam has a natural polarization). If the proton beam were to be polarized, it would be possible to measure polarization asymmetries and thus explore spin dependent structure functions along with the spin-independent structure functions in the HERA kinematic range. In this paper we discuss what might be achieved from such a programme. We show that the data HERA could provide are clearly unique and cannot be obtained by present day experiments.

In section 2 we estimate the data that could be obtained, including the statistical errors, from inclusive polarized e-p scattering with HERA in the collider mode. We also discuss systematic errors and argue that they can be controlled within adequate limits. In section 3 we

briefly review the relation of the structure function g_1 to polarized parton distributions and the perturbative evolution equations satisfied by the latter, and summarize the status of polarized parton distributions extracted from presently available fixed target data. In section 4 we show that new data from polarized colliding beam experiments at HERA would shed light on the small x behaviour of g_1 and would substantially improve the determination of the polarized gluon distribution.

2 Measurement of $g_1^p(x, Q^2)$ at HERA

2.1 Kinematic range and statistical errors for HERA data

Presently all measurements of polarized structure functions are made using fixed target deep inelastic lepton-nucleon scattering. Figure 2 shows the kinematic ranges in which polarized lepton-proton data have been obtained at SLAC and CERN as well as the possible measurements in the kinematic domain available at HERA with 800 and 25 GeV proton and electron beams, respectively. Note the large extension in $x - Q^2$ range compared to the present data. Table 1 lists the $x - Q^2$ values at which measurements can be made at HERA, the number of events that would be measured and the associated statistical errors in the measured asymmetry δA_m assuming an integrated luminosity of $L = 1000$ pb^{-1} and electron and proton polarizations of 0.7 each[3]. Kinematic cuts [11] on y and the scattered electron angle θ'_e used for data analysis by the H1 and ZEUS collaborations were applied for the evaluation of the counting rates in each $x - Q^2$ bin. Standard deep inelastic scattering formulae were used to calculate of the kinematics and asymmetries. They are given in the Appendix.

2.2 Systematic errors for HERA data

The systematic errors associated with spin dependent asymmetry measurements are of two types: 1) normalization errors and 2) false asymmetries.

The normalization errors include principally uncertainties in the electron polarization P_e and in the proton polarization P_p . These lead to a change in the magnitude of the measured asymmetry but in practice by an amount which is small compared to the statistical error, and hence they are important primarily when evaluating the first moment of $g_1^p(x)$.

Recently the HERMES collaboration has reported a measurement of P_e by Compton scattering, which yielded a relative accuracy of 5.5% [13]. It is expected that an improved accuracy will be achieved eventually.

Absolute measurement of the polarization of the high energy (800 GeV) proton beam presents a new challenge and is presently under investigation. Several methods are being considered:

1. $p - p$ elastic scattering in the Coulomb-nuclear interference region[14],

[3]Accelerator parameters that were suggested by R. Klanner and F. Willeke for this workshop.

x	Q^2 GeV^2	y	D	N_{total}	δA_m
5.6×10^{-5}	1.8	0.40	0.47	5.0×10^6	4.5×10^{-4}
1.8×10^{-4}	1.8	0.13	0.13	8.0×10^6	3.5×10^{-4}
	5.6	0.40	0.46	3.5×10^6	5.3×10^{-4}
5.6×10^{-4}	1.8	0.04	0.04	1.2×10^7	2.9×10^{-4}
	5.6	0.13	0.13	6.5×10^6	3.9×10^{-4}
	1.8×10^1	0.40	0.47	2.0×10^6	7.1×10^{-4}
1.8×10^{-3}	1.8	0.01	0.01	1.6×10^7	2.5×10^{-4}
	5.6	0.04	0.04	9.0×10^6	3.3×10^{-4}
	1.8×10^1	0.13	0.13	3.4×10^6	5.4×10^{-4}
	5.6×10^1	0.40	0.47	1.1×10^6	9.5×10^{-4}
5.6×10^{-3}	5.6	0.01	0.01	1.2×10^7	2.8×10^{-4}
	1.8×10^1	0.04	0.04	5.5×10^6	4.3×10^{-4}
	5.6×10^1	0.13	0.13	1.7×10^6	7.7×10^{-4}
	1.8×10^2	0.40	0.47	5.5×10^5	1.3×10^{-3}
1.8×10^{-2}	1.8×10^1	0.01	0.01	6.5×10^6	3.9×10^{-4}
	5.6×10^1	0.04	0.04	2.6×10^6	6.2×10^{-4}
	1.8×10^2	0.12	0.13	8.0×10^5	1.1×10^{-3}
	5.6×10^2	0.40	0.47	2.3×10^5	2.1×10^{-3}
5.6×10^{-2}	5.6×10^1	0.01	0.01	2.2×10^6	6.7×10^{-4}
	1.8×10^2	0.04	0.04	8.0×10^5	1.1×10^{-3}
	5.6×10^2	0.12	0.13	2.6×10^5	2.0×10^{-3}
	1.8×10^3	0.40	0.47	6.5×10^4	3.9×10^{-3}
1.8×10^{-1}	1.8×10^2	0.01	0.01	5.9×10^5	1.3×10^{-3}
	5.6×10^2	0.04	0.04	1.9×10^5	2.3×10^{-3}
	1.8×10^3	0.13	0.13	5.4×10^4	4.3×10^{-3}
	5.6×10^3	0.40	0.47	1.3×10^4	8.6×10^{-3}
5.6×10^{-1}	5.6×10^2	0.01	0.01	2.9×10^4	5.9×10^{-3}
	1.8×10^3	0.04	0.04	8.3×10^3	1.1×10^{-2}
	5.6×10^3	0.13	0.13	1.9×10^3	2.3×10^{-2}
	1.8×10^4	0.40	0.47	4.2×10^2	4.8×10^{-2}

Table 1: *The kinematic variables x, Q^2, y, and D, along with the number of events expected N_{total}, and the statistical uncertainty in the measured asymmetry δA_m in the kinematical region assuming an integrated luminosity $L = 1000\ pb^{-1}$ and proton and electron beam polarizations $P_p = P_e = 0.7$.*

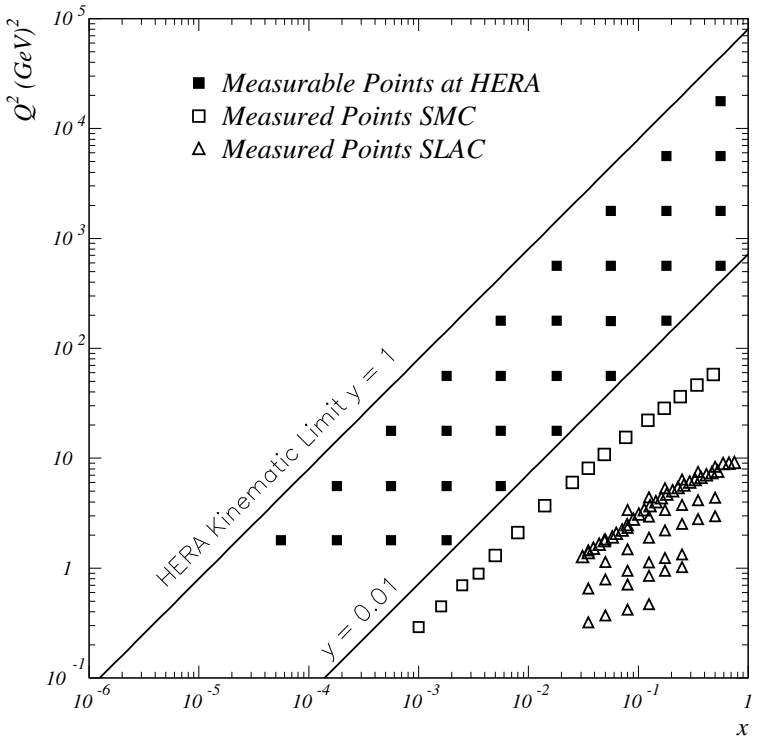

Figure 2: *Measurable $x - Q^2$ region at HERA shown with the presently explored regions by SMC(CERN) and E143(SLAC) experiments, and the kinematic limit of measurability at HERA.*

2. $p - \vec{\mathrm{p}}$ scattering using a stationary polarized proton jet target and comparing the asymmetries $A_{\mathrm{beam}} = A_{\mathrm{jet}}$, where A_{beam} is the asymmetry in the scattering of the polarized beam from an *unpolarized* jet and A_{jet} is the asymmetry measured with an *unpolarized* beam and a polarized jet target with a known polarization P_{jet}. Adjusting the jet polarization to obtain the same asymmetry, one obtains the beam polarization $P_{\mathrm{beam}} = P_{\mathrm{jet}}$ [15].
3. polarized $e - p$ scattering in which a low energy polarized electron beam collides with the polarized 800 GeV proton beam, with kinematics corresponding to the polarized $e-p$ elastic scattering measurements at SLAC [16]. The theoretical values for the asymmetry in elastic scattering are given in terms of the polarizations and the measured electric and magnetic form factors of the proton. Hence the measured asymmetry at HERA using a known polarized electron beam would determine P_p.

We comment briefly on these possible methods. For method 1 the nuclear matrix element may not be known well enough to provide a significant absolute determination of P_p. Method 2 appears quite attractive because only the invariance principle is needed from theory, and it may be possible to use the stationary polarized target of the HERMES experiment for this measurement. Method 3 is theoretically sound and simple, but may not be attractive experimentally. These methods have still to be fully developed and tested experimentally. It is reasonable to expect that a 5% accuracy will be achieved.

Inclusive π^+ or π^- production in collisions of 800 GeV protons with a fixed proton target appears to be a simple method for a relative measurement of the polarization [17].

Methods to measure P_p are presently considered and studied also for polarized protons at RHIC. The method of measuring P_p at 1 TeV has been discussed in some detail in a design report entitled "Acceleration of Polarized Protons to 120 GeV and 1 TeV at Fermilab" [18] as well as in the BNL proposal for RHIC SPIN [19].

The other type of systematic error comes from false asymmetries. These arise from variations in counting rate due to time variations in detector efficiencies, beam intensities, or crossing angles between the conditions of spins parallel and antiparallel. In view of the expected small values of the true asymmetries expected in the HERA kinematic region, (Table 1), the false asymmetries must be controlled at the level of 10^{-4}. We note that medium and high energy experiments which have measured parity violation have controlled false asymmetries to less than 10^{-5} to 10^{-8} [20].

False asymmetries can be avoided by frequent reversals of spin orientations. In the HERA collider the electron(positron) spin reversal is difficult and time consuming (several hours) and would lead to changes in beam intensity and beam emittance. Hence asymmetry data must be obtained with a fixed helicity for the electron beam by varying the proton helicity. Both the electron and proton rings are filled with about 200 particle bunches. The proton ring can be filled with bunches of protons with individually predetermined polarizations. Parallel and antiparallel spin data would be obtained at successive beam crossings occurring at time intervals of about 100 ns. Such alternations eliminate many errors in an asymmetry measurement. However, differences in the intensities and the crossing angles at successive proton bunches could still lead to false asymmetries and will have to be minimized.

The most important approach to avoid false asymmetries will be to use a spin rotator to reverse the helicity of all proton bunches at adequately frequent intervals (perhaps once per 8 hours). The design of such rotators has been studied and appears practical without appreciable change in the orbits, or in the magnitude of proton polarization [21]. Studies at the IUCF at 370 MeV have confirmed these conclusions [22]. With such approach the false asymmetries could be controlled to less than 10^{-4}.

3 Current status of $g_1(x, Q^2)$

3.1 Perturbative evolution of $g_1(x, Q^2)$

The definition and properties of the polarized structure function g_1 in perturbative QCD closely parallel that of its unpolarized counterpart F_2 (see ref. [23] for a review). The structure function g_1 is related to the polarized quark and gluon distributions through

$$\begin{aligned} g_1(x,t) &= \tfrac{1}{2}\langle e^2\rangle \int_x^1 \frac{\mathrm{d}y}{y}\Big[C_q^{\mathrm{S}}(\tfrac{x}{y},\alpha_s(t))\Delta\Sigma(y,t) \\ &+ 2n_f C_g(\tfrac{x}{y},\alpha_s(t))\Delta g(y,t) + C_q^{\mathrm{NS}}(\tfrac{x}{y},\alpha_s(t))\Delta q^{\mathrm{NS}}(y,t)\Big], \end{aligned} \tag{1}$$

where $\langle e^2\rangle = n_f^{-1}\sum_{k=1}^{n_f} e_k^2$, $t = \ln(Q^2/\Lambda^2)$, $\Delta\Sigma$ and Δq^{NS} are the singlet and non-singlet polarized quark distributions

$$\Delta\Sigma(x,t) = \sum_{i=1}^{n_f}\Delta q_i(x,t), \qquad \Delta q^{\mathrm{NS}}(x,t) = \sum_{i=1}^{n_f}(e_i^2/\langle e^2\rangle - 1)\Delta q_i(x,t),$$

and $C_q^{S,NS}(\alpha_s(Q^2))$ and $C_g(\alpha_s(Q^2))$ are the quark and gluon coefficient functions.

The x and Q^2 dependence of the polarized quark and gluon distributions is given by Altarelli-Parisi equations [24]:

$$\frac{\mathrm{d}}{\mathrm{d}t}\Delta\Sigma(x,t) = \frac{\alpha_s(t)}{2\pi}\int_x^1 \frac{\mathrm{d}y}{y}\left[P_{qq}^{\mathrm{S}}(\tfrac{x}{y},\alpha_s(t))\Delta\Sigma(y,t) + 2n_f P_{qg}(\tfrac{x}{y},\alpha_s(t))\Delta g(y,t)\right], \quad (2)$$

$$\frac{\mathrm{d}}{\mathrm{d}t}\Delta g(x,t) = \frac{\alpha_s(t)}{2\pi}\int_x^1 \frac{\mathrm{d}y}{y}\left[P_{gq}(\tfrac{x}{y},\alpha_s(t))\Delta\Sigma(y,t) + P_{gg}(\tfrac{x}{y},\alpha_s(t))\Delta g(y,t)\right], \quad (3)$$

$$\frac{\mathrm{d}}{\mathrm{d}t}\Delta q^{\mathrm{NS}}(x,t) = \frac{\alpha_s(t)}{2\pi}\int_x^1 \frac{\mathrm{d}y}{y}\,P_{qq}^{\mathrm{NS}}(\tfrac{x}{y},\alpha_s(t))\Delta q^{\mathrm{NS}}(y,t), \quad (4)$$

where P_{ij} are polarized splitting functions.

The full set of coefficient functions [25] and splitting functions [26] has been computed up to next-to-leading order in α_s. As in any perturbative calculation, at next-to-leading order splitting functions, coefficient functions and parton distributions depend on renormalization and factorization scheme, while of course physical observables, such as g_1 itself, remain scheme-independent up to terms of order α_s^2. The scheme choice is arbitrary, and in particular parton distributions in different factorization schemes are related to each other by well-defined linear transformations.

The factorization scheme dependence is particularly subtle in the polarized case because of the extra ambiguity related to the definition of the γ_5 matrix, i.e. to the way chiral symmetry is broken by the regularization procedure. This is reflected in an ambiguity in the size of the first moment of the gluon coefficient function C_g (which starts at order α_s). Two widely adopted choices [8, 27, 28], both compatible with the choice of $\overline{\mathrm{MS}}$ renormalization and factorization, correspond to either requiring the first moment of the gluon coefficient function to be $C_g^1 = 0$, or imposing that the first moment of the polarized quark distribution be scale independent, which implies $C_g^1 = -\frac{\alpha_s}{4\pi}$. The first moment Δg^1 of the gluon distribution can be chosen to be the same in the two schemes, whereas the first moments of the quark distribution in the two schemes differ by an amount proportional to $\alpha_s\Delta g^1$. Because the evolution equations 2-4 imply that at leading order the first moment of the polarized gluon scales as $\frac{1}{\alpha_s}$ this scheme dependence persists asymptotically and is potentially large if the first moment of the gluon distribution is large [29].

3.2 Current status of polarized parton distributions.

Parton distributions can be extracted from experimental structure function data by parametrizing them at a starting value of Q^2, evolving this initial condition up to any desired value of x and Q^2 using Eqs. 2-4, determining g_1 there by means of Eq. 1, and determining the initial parametrization which gives the best fit of $g_1(x,Q^2)$ to the data [8, 27, 28]. Here we follow the procedure used in refs. [8, 30]: we give the initial conditions at $Q^2 = 1$ GeV^2 in the form

$$\Delta f(x,Q^2) = N(\alpha_f,\beta_f,a_f)\ \eta_f\ x^{\alpha_f}(1-x)^{\beta_f}(1+a_f\ x), \quad (5)$$

where $N(\alpha,\beta,a)$ is fixed by the normalization condition, $N(\alpha,\beta,a)\int_0^1 dx x^{\alpha}(1-x)^{\beta}(1+ax) = 1$, and Δf denotes $\Delta\Sigma$, Δq_{NS}, or Δg. With this normalization the parameters η_g, η_{NS}, and η_S are respectively the first moments of the gluon, the non-singlet quark and the singlet quark

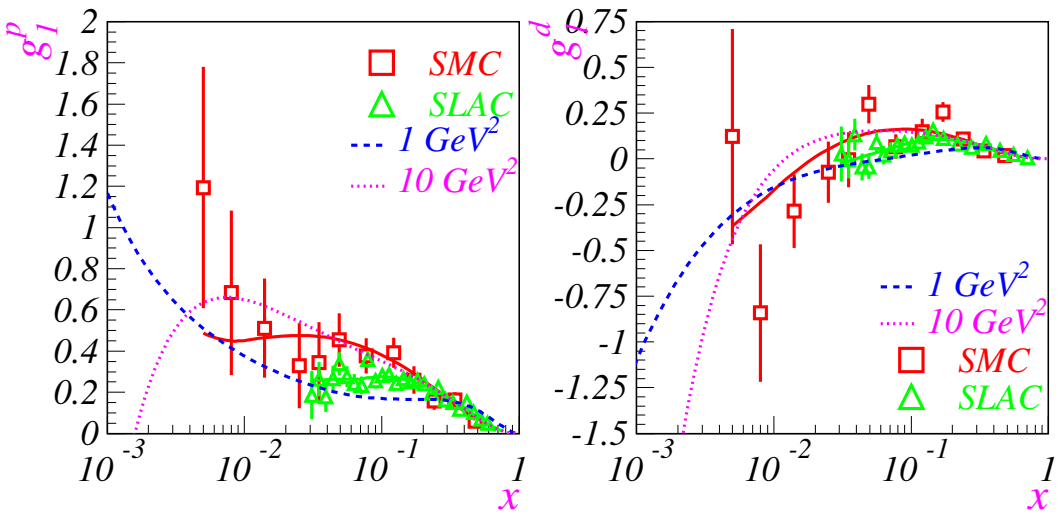

Figure 3: *The NLO fit to proton g_1^p and deuteron g_1^d data. The solid lines are fits to data at the measured Q^2 values, and the dashed and the dotted lines are fits evolved to $Q^2 = 1$ and 10 GeV^2 respectively.*

distributions at the starting scale. Evolution is performed within the AB factorization scheme (which has $C_g^1 = -\frac{\alpha_s}{4\pi}$). Further details of the fits and analysis are given in ref. [8, 30].

Using the published data on proton and deuteron structure functions by SMC [6], and E143 [7] the best fit results obtained for such analysis [8] are given in column 1 of Table 2. The data used for the analysis and the results of the NLO fit are shown in Fig. 3. Interestingly, the data require the first moment of the gluon distribution to differ significantly from zero: $\eta_g = 1.52 \pm 0.74$. This result follows mostly from the observed scaling violations in the intermediate and small x region. However, the statistical uncertainty on the size of the polarized gluon distribution is still rather large. Moreover, existing data only partially constrain the small x behaviour of the various parton distributions (values of α_S, α_g, and α_{NS}), and do not allow a precise determination of their asymptotic form for small x. Such information, besides its intrinsic theoretical interest, is required in order to obtain a precise determination of the moments of g_1 [8, 30]. New data with an extended kinematic coverage in x and Q^2 provided by HERA could reduce these uncertainties.

Since the publication of ref. [8], new data on the Q^2 dependence of g_1 have been published by the E143 collaboration. The inclusion of these data in the NLO fits results in reduction of up to 20% in the errors on the fitted parameters, all the values of the parameters being consistent with the published values. The value of the first moment of the gluon distribution at $Q^2 = 1$ GeV^2 for example becomes $\eta_g = 1.29 \pm 0.56$. In the next two years both SMC (CERN) and E143 (SLAC) plan to present new data on proton and deuteron spin structure functions and using these data as well a more accurate determination of the parameters in the fit can be expected. It can thus be anticipated that eventually the dominant uncertainty in the determination of the first moments of g_1 and the polarized gluon distribution will be due to lack of experimental information in the HERA region.

4 The impact of polarized HERA data

4.1 The small x behaviour of g_1

As shown in Fig. 2, measurements of g_1 at HERA will extend the x region down to $x = 5.6\times10^{-5}$. Knowledge of the small x behaviour of g_1 is obviously necessary in order to compute moments of g_1, and indeed in the determination of the singlet component of the first moment of g_1 the uncertainty related to the lack of knowledge of this behaviour is already comparable to the statistical uncertainty [8, 30].

The extrapolation of g_1 from the measured region down to $x = 0$ is traditionally done by assuming Regge behaviour of the structure function, which implies [31] $g_1 \sim x^\alpha$ as $x \to 0$ with $0 \leq \alpha \leq 0.5$, i.e. a valence-like behaviour of g_1. This behaviour seems to disagree with the data (see Table 2 and Fig. 3) which suggest instead that both the singlet and nonsinglet components of g_1 rise at small x.

In fact, a valence-like behaviour of g_1 is incompatible with perturbative QCD, which at leading order predicts instead that g_1 should rise at least as $g_1(x,Q^2) \sim \frac{1}{\sqrt{\sigma}} e^{2\gamma\sigma}$, where $\sigma \equiv \sqrt{\xi\zeta}$, $\rho \equiv \sqrt{\xi/\zeta}$, $\xi \equiv \ln\frac{x_0}{x}$, $\zeta \equiv \ln\frac{\alpha_s(Q_0^2)}{\alpha_s(Q^2)}$, and Q_0 and x_0 are reference values of x and Q^2. This rise is present both in the singlet and nonsinglet components of g_1, but with different slopes γ, calculable in perturbative QCD. The sign of this rise depends on the specific form of the quark and gluon distributions, but for most reasonable forms of Δq and Δg, and in particular if Δg at moderately small x is positive definite, then g_1 will be negative. The onset of this behaviour as Q^2 is raised is clearly shown in Fig. 3. Higher order corrections lead to an even stronger drop: at k-th perturbative order the rise of $-g_1$ is enhanced by a factor of $\alpha_s^k\rho^{2k+1}$. It has been suggested [32] that these terms to all orders in α_s may exponentiate, thus leading to a rise of g_1 as a power of x; the sign of this rise is still predicted to be negative.

A non-Regge behaviour of the unpolarized structure function F_2 has been observed and accurately measured at HERA, in spectacular agreement with the perturbative QCD prediction [11, 12]. The behaviour correspondingly predicted in the polarized case is even more interesting due to the fact that higher order corrections are stronger, and also the polarized singlet and nonsinglet quark and gluon distributions all display qualitatively the same behaviour, whereas in the unpolarized case only the gluon dominates at small x.

An experimental measurement of the small x behaviour of g_1 would thus lead to significant insight on the structure of QCD both within and beyond perturbation theory. In Fig. 4 we show the expected accuracy of the determination of g_1 at HERA within the maximal extent of variation in the small x behaviour compatible with the requirement of integrability of g_1 (which implies that at small x g_1 can rise at most as $1/(x\ln^\alpha x)$ with $\alpha > 1$).

The full coverage of HERA experiments is shown in Figs. 5, 6, 7, and 8, where projected data with their estimated errors are given on the basis of the NLO fit of Table 2. The errors are estimated assuming integrated luminosities $L = 1000\ pb^{-1}$ and beam polarizations $P_p = P_e = 0.7$. In Fig. 5 g_1 at the starting scale $Q^2 = 1$ GeV^2 is shown using the best fit values of the parameters. This is then evolved up with different choices for the normalization of the polarized gluon distribution, to give a feeling for the possible range of variation. In particular, we consider two cases: a) the first moment of the gluon distributions is fixed to be 0 at Q^2 = 1 GeV^2 (minimal gluon: dashed lines in Fig.6) and b) the first moment of the singlet quark density was fixed to $\eta_q = a_8$ at the same reference scale (maximal gluon: dotted lines in Fig.6).

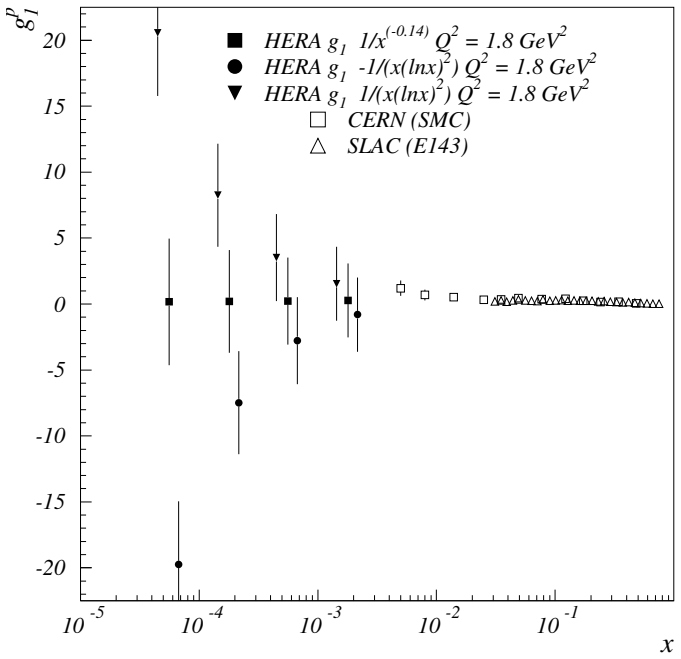

Figure 4: *The structure function g_1^p measurable at HERA for $Q^2 = 1.8$ GeV^2 with integrated luminosity $L = 1000$ pb^{-1} are shown. The SMC and E143 measurements are shown for comparison. Starting from the measured values of g_1^p by SMC, the measurable values for HERA at low-x are shown in two extreme cases: valence-like behaviour $g_1(x) \sim x^{-\alpha}$ with $\alpha = 0.14$ or strong powerlike positive or negative rises $g_1(x) \sim \pm 1/(x \cdot (lnx)^2)$*

Even though the current best fit value of η_g (Table 2) is very close to the maximal case, the minimal gluon is at present only excluded at 2 σ level. Of course yet wider deviations from these fits are foreseeable since the small x behaviour of the current best fit is only very loosely constrained due to the lack of direct experimental information at small x; also, as discussed above, higher order corrections beyond NLO may turn out to be important at very small x.

In Fig. 6 we show the statistical errors for each measurable data point in the complete $x - Q^2$ grid indicated in Fig. 2 and in Table 1. The bold solid lines are the predictions of g_1 values in the HERA kinematic range using the best fit values of the NLO parameters for the presently published data [6, 7]. In Fig. 7 the projected values of g_1 obtained from the NLO fit to the data are calculated for the lowest Q^2 data point reached at that x bin, which in turn has the lowest statistical error. The Q^2 values are indicated in the figure. The measured asymmetries A_m and the corresponding statistical errors on the projected measurements at HERA at different Q^2 are shown in Fig. 8.

4.2 The determination of the gluon distribution

The measurement of scaling violations in inclusive structure functions provides a theoretically clean determination of the polarized gluon distribution. Because the gluon distribution is only determined by the scale dependence of the moments of g_1 a reasonably wide kinematic coverage is required in order to achieve such a determination with satisfactory accuracy: in particular, since the gluon distribution is peaked at small x, data in this region for several values of Q^2 such as those obtainable at HERA would substantially improve the determination of $\Delta g(x, Q^2)$.

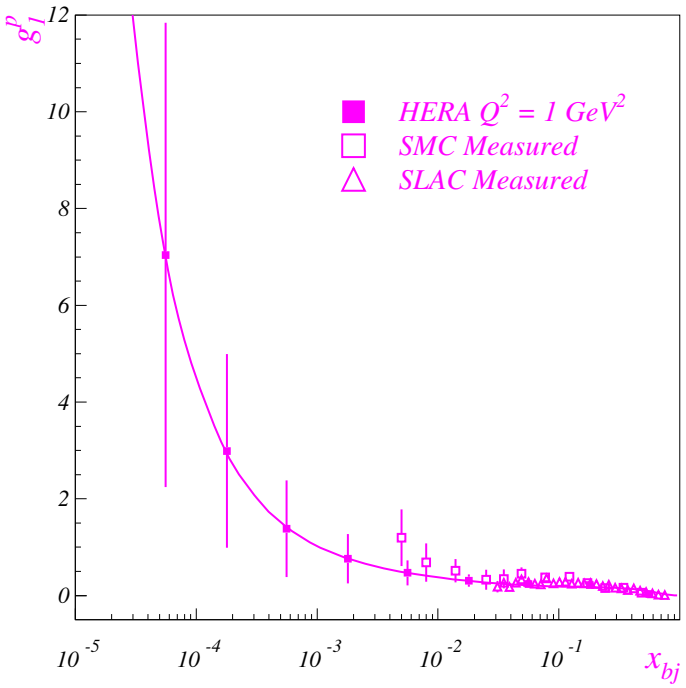

Figure 5: *The starting parametrization of g_1^p at $Q^2 = 1$ GeV^2 which gives best-fit to present-day data is shown in the x range covered at HERA. Statistical errors on g_1 after combining all measurements for each x are shown for an integrated luminosity $L = 1000$ pb^{-1}.*

To assess the impact of these data we have repeated the fit described in sect. 3.2 with the addition of the projected HERA data discussed in sect. 2.1. The values of the best-fit parameters of course do not change, but using the estimated errors from acceptance considerations on measurable g_1, we get an estimate of the extent of reduction in the measured uncertainties of various parameters. In column 3 of Table 2 we show the results of a fits with HERA data for integrated luminosity $L = 1000$ pb^{-1} and in column 4 we show the results for $L = 200$ pb^{-1}. Note in particular the sizable improvement in the determination of the first moment of Δg, which is of greatest theoretical interest due to its role in the understanding of the proton spin structure [5]: from $\delta(\Delta g^1) = \pm 0.74$ (the present value) to ± 0.22 or ± 0.28 depending on the luminosity available at HERA.

We have also performed fits with an additional parameter in the distribution functions of Eq. 5

$$\Delta f(x, Q^2) = N(\alpha_f, \beta_f, a_f)\ \eta_f\ x^{\alpha_f}(1-x)^{\beta_f}(1 + a_f\ x + b_f\ \sqrt{x}), \tag{6}$$

(i.e. a 14 parameter fit), in order to test the sensitivity of our results to the functional form used for the parton distributions. The fits yielded a result for $\eta_g = 1.0 \pm 0.3$ consistent with the 10 parameter fit.

5 Conclusions

Inclusive DIS measurements at HERA with high integrated luminosity with high energy polarized electrons and polarized protons would yield significant and unique new information on

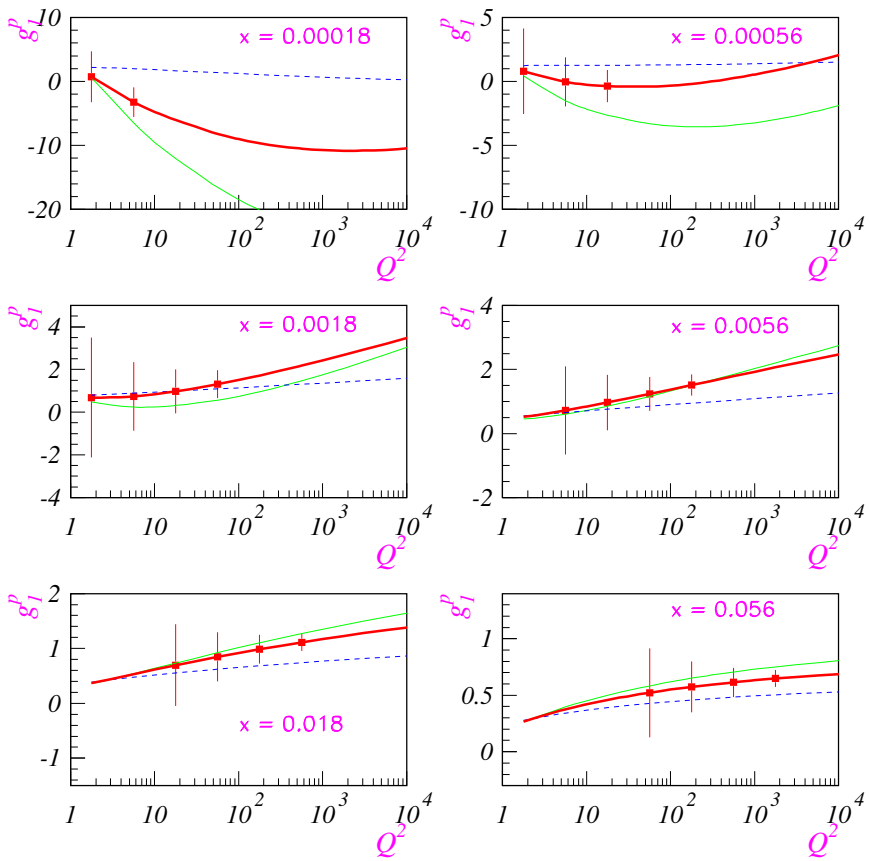

Figure 6: *Predicted values for g_p^1 from NLO fits together with estimated statistical uncertainties for a future polarized DIS experiment with an integrated luminosity L=1000 pb^{-1}. The solid bold lines are predictions based on fits to SMC and SLAC data extended in to the HERA kinematic range while the dotted and dashed lines are the maximal and minimal gluon predictions (see text).*

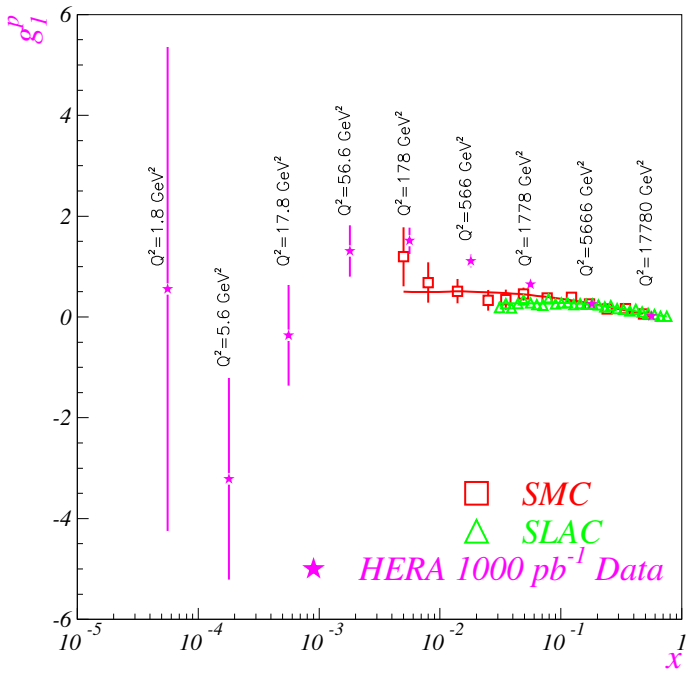

Figure 7: *The structure function g_1^p measurable at HERA shown in comparison to the SMC/E143 measurements. The values of $g_1^p(x, Q^2)$ for each measurable HERA point are taken from the NLO fit and evolved to the Q^2 value indicated in the figure. Statistical errors on $g_1(x)$ averaged over all Q^2 for measurements at HERA with integrated luminosity L = 1000 pb^{-1} are shown for each x.*

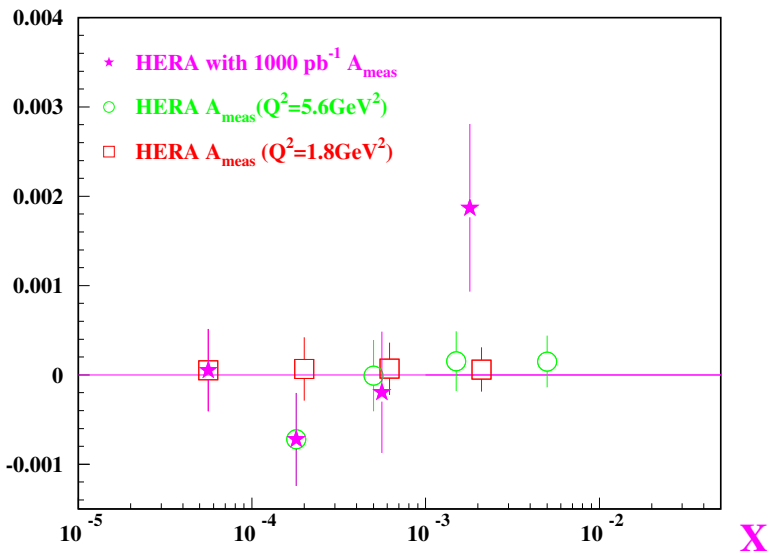

Figure 8: *The measured asymmetry A_m for different Q^2 at HERA for the projected data points shown in previous figures.*

Parameter	Published Best Fit	HERA $L = 1000\ pb^{-1}$	HERA $L = 200\ pb^{-1}$
η_g	1.52±0.74	1.29±0.22	1.29±0.28
η_q	0.48±0.09	0.45±0.04	0.45±0.05
η_{NS}	Fixed	Fixed	Fixed
α_g	-0.47±0.30	-0.64±0.11	-0.64±0.16
α_q	0.41±0.38	0.42±0.26	0.42±0.30
α_{NS}	-0.68±0.15	-0.73±0.10	-0.73±0.12
β_g	2.6±4.8	4.0 (fixed)	4.0 (fixed)
β_q	3.3±1.4	3.50±0.81	3.50±1.13
β_{NS}	2.2±0.3	2.10±0.14	2.10±0.27
$a_q = a_g$	0.1±3.0	1.2±2.5	1.2±2.10
a_{NS}	16.0±17.0	19.5±14.0	19.5±16.4

Table 2: *Results of NLO fits: Column 2 for the published results for data available in 1995, Column 3: estimated results for the available data in 1996 and data at HERA with integrated luminosity $L = 1000\ pb^{-1}$, and Column 4: estimated results using available data in 1996 and the data at HERA with $L = 200\ pb^{-1}$. The parameter η_{NS} is not fitted, its value is taken from hyperon β decay measurements.*

$g_1^p(x, Q^2)$ over a much extended range in x and Q^2. For such measurements the false asymmetries should be considerably smaller than the true asymmetries to be measured, and normalization systematic errors should be controlled to be less than 10%. Statistical errors on the points will dominate.

There is a strong and broad current interest in the spin structure of the nucleon. Proposals have been made and experiments are planned to study this problem at several accelerator facilities. These include COMPASS at CERN, a possible experiment at SLAC, and RHIC SPIN at BNL. A principal goal of all of these proposed experiments is to measure the polarized gluon content in the nucleon from a study of semi-inclusive processes. Another experiment involving a semi-inclusive process is discussed in this volume where the determination of Δg from a study of dijets from polarized e-p collisions at HERA is described. A measurement of Δg from inclusive process has the advantage of being theoretically clean, but requires a wide kinematic coverage in x and Q^2, and could thus only be performed at HERA.

The inclusive measurements with HERA discussed in this chapter will also provide unique information on the behaviour $g_1^p(x, Q^2)$ over an unexplored kinematic range, which is of great theoretical interest.

The fact that HERA is an operating facility with a plan for substantial increase in luminosity and with two major operating detectors, as well as a polarized electron beam, means that only the high energy polarized proton beam needs to be developed. The efforts to achieve that seem well justified and data from such experiments at HERA would provide unique and complementary information to that from other presently proposed experiments.

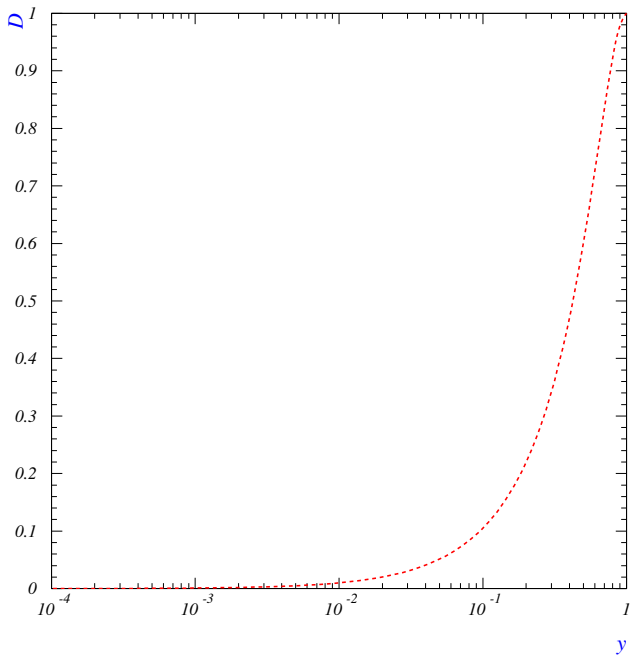

Figure 9: *The dependence of depolarization factor D on y.*

6 Appendix: Kinematics of polarized DIS at HERA

The polarized structure function g_1^p of the proton is related to the virtual photon asymmetry A_1^p by the relation [33],

$$g_1 = \frac{F_2}{2x(1+R)} A_1 \tag{7}$$

in terms of the unpolarized structure function F_2 and the ratio of longitudinal to transverse photoabsorption cross sections R.[4]. The measured longitudinal asymmetry A_m is related to A_1 by,

$$A_m = \frac{N^{\uparrow\uparrow} - N^{\uparrow\downarrow}}{N^{\uparrow\uparrow} + N^{\uparrow\downarrow}} = P_p P_e D A_1 \tag{8}$$

where $P_p(P_e)$ is the proton (electron) polarization, and D is the depolarization factor. The arrows indicate the relative direction of the spins of the electrons and protons. D is calculable from QED and is given by

$$D = \frac{y(2-y)}{y^2 + 2(1-y)(1+R),} \tag{9}$$

where

$$y = \frac{Q^2}{xs} \tag{10}$$

and s is the Mandelstam invariant of the electron-proton collision. The dependence of D on y is shown in Fig. 9. The statistical uncertainty δA_m in the measurement of A_m is given by,

$$\delta A_m = \frac{1}{\sqrt{N^{\uparrow\uparrow} + N^{\downarrow\uparrow}}} = \frac{1}{\sqrt{N_{total}}} \tag{11}$$

[4]This result holds at leading twist.

where $N^{\uparrow\uparrow}$ $^{(\uparrow\downarrow)}$ represent the number of DIS events observed with parallel (anti parallel) proton and electron polarizations, respectively. The sum in the denominator is then the square root of the total number of events observed in the experiment at selected $x - Q^2$ bins.

We estimate the yield and the associated statistical error to be observed in a future HERA experiment. The cross section for DIS is given by

$$\frac{d^2\sigma}{dxdQ^2} = \frac{4\pi\alpha^2}{xQ^4}\left[1 - y + \frac{y^2}{2(1+R)}\right]F_2 \tag{12}$$

The depolarization factor D for each of the bins was calculated and used to estimate the statistical uncertainty in the measurement of g_1^p from Eqs. 9 and 11.

Acknowledgements: We thank G. Altarelli and P. Schuler for interesting discussions and helpful comments.

References

[1] R. Hofstadter, Rev. Mod. Phys. **28** (1956) 214.

[2] J. Friedman et al., Ann. Rev. Nucl. Science **22**, (1972), 203.

[3] SLAC E80, M. J. Alguard et al., Phys. Rev. Lett. **37** (1976) 1261; ibid **41** (1978) 70;
SLAC E130, G. Baum et al., Phys. Rev. Lett. **51** (1983) 1135.

[4] EMC, J. Ashman et al., Nucl. Phys. **B328** (1989) 1.

[5] See e.g. G. Altarelli and G. Ridolfi, Nucl. Phys. B Proc. Suppl. **39B** (1995) 106;
R. D. Ball, `hep-ph/9511330`, in the proceedings of the Erice school on nucleon spin structure;
S. Forte, `hep-ph/9511345`, in the proceedings of the 7th Rencontres de Blois.

[6] SMC, B. Adeva et al., Phys. Lett. **B302** (1993) 533;
SMC, D. Adams et al., Phys. Lett. **B329** (1994) 399;
SMC, D. Adams et al., Phys. Lett. **B357** (1995) 248.

[7] E-143, K. Abe et al., Phys. Rev. Lett. **74** (1995) 346;
E-143, K. Abe et al., Phys. Rev. Lett **75** (1995) 25.

[8] R. D. Ball, S. Forte and G. Ridolfi, Phys. Lett. **B378** (1996) 255.

[9] M. Klein, H1 Collaboration, in "DIS 96" (World Scientific, 1996).

[10] R. Yoshida, ZEUS Collaboration, in "DIS 96" (World Scientific, 1996).

[11] A. De Roeck, lectures at the 1994 Cargèse school, preprint DESY-95-025.

[12] R.D. Ball and A. De Roeck, in "DIS96" (World Scientific, 1996).

[13] HERMES Collaboration, in "DIS96" (World Scientific, 1996).

[14] N. Akchurin et al., Phys. Rev. **D48** (1993) 3026.

[15] L. Wolfenstein, Ann. Rev. Nuclear Science **6** (1956) 43.

[16] M. J. Alguard et al., Phys. Rev. Lett. **37** (1976) 1258.

[17] D. Adams et al., Phys. Lett. **B246** (1991) 14.

[18] "Acceleration of Polarized Protons to 120 GeV and 1 TeV at Fermilab", Univ. of Michigan, HE 95-09, (July 1995).

[19] RHICSPIN proposal

[20] C. Y. Prescott et al., Phys. Lett. **B77** (1978) 347; Phys. Lett. **B84** (1979) 524.
V. Yuan et al., Phys. Rev. Lett. **57** (1986) 320 (and references therein);
P. A. Souder et al., Phys. Rev. Lett. **65** (1990) 694.

[21] T. Roser, Nucl. Instr. Meth. **A342** (1994) 343.

[22] R. A. Phelps et al., Phys. Rev. Lett. **72** (1994) 1479.

[23] G. Altarelli, Phys. Rep. **81** (1982) 1.

[24] G. Altarelli and G. Parisi Nucl. Phys. **B126** (1977) 298.

[25] J. Kodaira et al., Phys. Rev. **D20** (1979) 627.

[26] R. Mertig and W.L. van Neerven, Z. Phys. **C70** (1996) 637;
W. Vogelsang, preprint RAL-TR-96-020, hep-ph/9603366 (1996).

[27] W. J. Stirling and T. Gehrmann, Z. Phys. **C65** (1995) 461; Phys. Rev. **D53** (1996) 6100.

[28] M.Glück, E. Reya, M. Stratmann and W. Vogelsang, Phys. Rev. **D53** (1996) 4775 .

[29] G. Altarelli and G. G. Ross, Phys. Lett. **B212** (1988) 391;

[30] R. D. Ball, S. Forte and G. Ridolfi, Nucl. Phys. **B444** (1995) 287.

[31] R. L. Heimann, Nucl. Phys. **B64** (1973) 429.

[32] R. Kirschner and L. Lipatov, Nucl. Phys. **B213** (1983) 122;
J. Bartels, B. I. Ermolaev and M. G. Ryskin, Z. Phys. **C70** (1996) 273; preprint DESY-96-025, `hep-ph/9603204`

[33] T. Pussieux and R. Windmolders, "A Collection of Formulas for Spin Dependent Deep Inelastic Scattering", DAPNIA-SPHN-95-10, also in "Internal Spin Structure of the Nucleon", Edited by V. W. Hughes, C. Cavata, p212, (World Scientific, Singapore 1995).